New cosmological constraints to find plausible dark energy candidates

Luz Ángela García

Universidad ECCI

Work done in collaboration with Prof. Leonardo Castañeda (OAN)

Current challenges in cosmology

* Does DE really exist? If it does, how can we detect it?

* Is CC a real representation of DE? → Fundamental nature of CC: high energy physics match?

*Many (correlated) observables: CMB, lensing, galaxy clustering, SN, clusters, etc.

* Different theoretical models: e.g. SN light curve fitters, bias models for galaxy clustering, …

* Each probe contains its own nuisance parameters, and fitting models.

* Different parameters & systematics in each model: hard to track samples over each MCMC chain.

*Complex multimodal posterior & likelihoods: sampling choice end up having a non-null impact in the results, estimate/model covariances.

Gravity/Dark Energy: a cornucopia of models

The most broadly studied models are of the form

$$S = \int \mathrm{d}^4x\sqrt{-g}\left[\frac{\mathcal{R}}{16\pi G} + \mathcal{L}_\mathrm{m} + \frac{\Lambda}{8\pi G}\right], \quad \text{GR + LCDM}$$

$$S = \int \mathrm{d}^4x\sqrt{-g}\left[\frac{\mathcal{R}}{16\pi G} + \mathcal{L}_\mathrm{m} + \frac{1}{2}\nabla^\mu\varphi\nabla_\mu\varphi + V(\varphi)\right], \text{ free quintessence}$$

$$S = \int \mathrm{d}^4x\sqrt{-g}\left[\frac{\mathcal{R}}{16\pi G} + \mathcal{L}_\mathrm{m}\left(A(\varphi), g_{\mu\nu}\right) + \frac{1}{2}\nabla^\mu\varphi\nabla_\mu\varphi + V(\varphi)\right],$$

$$S = \int \mathrm{d}^4x\sqrt{-g}\left[\frac{\mathcal{R}}{16\pi G} + \mathcal{L}_\mathrm{m} + f(\mathcal{R})\right], \quad \text{Coupled quintessence/f(R)}$$

$$S = \int \mathrm{d}^4x\sqrt{-g}\left[\frac{\mathcal{R}}{16\pi G} + \mathcal{L}_\mathrm{m} + \nabla^\mu\varphi\nabla_\mu\varphi\left(\frac{c_2}{2} + \frac{c_3}{2\mathcal{M}^3}\Box\varphi\right)\right], \quad \text{galileon}$$

$$S = \int \mathrm{d}^4x\sqrt{-g}\left[\frac{\mathcal{R}}{16\pi G} + \mathcal{L}_\mathrm{m}\left(A(\varphi), g_{\mu\nu}\right) + K\left(\nabla_\mu\varphi\nabla^\mu\varphi\right)\right], \quad \text{“K-essence”}$$

$$S = \int \mathrm{d}^4x\sqrt{-g}\left[\frac{\mathcal{R}}{16\pi G} + \mathcal{L}_\mathrm{m} + f\left(\Box^{-n}\mathcal{R}\right)\right], \quad \text{“Non-local gravity”}$$

$$S = \int \mathrm{d}^4x\sqrt{-g}\left[\frac{\mathcal{R}}{16\pi G} + \mathcal{L}_m\right] + \int \mathrm{d}^5x^{(5)}\sqrt{g^{(5)}}\left[\frac{\mathcal{R}^{(5)}}{16\pi G^{(5)}}\right], \quad \text{“Brane-world” or extra dimensions}$$

See Yoo+ 2012, Tawfik+ 2019, Ferreira 2019 for a detailed review of the models.

Constraining cosmo parameters given data

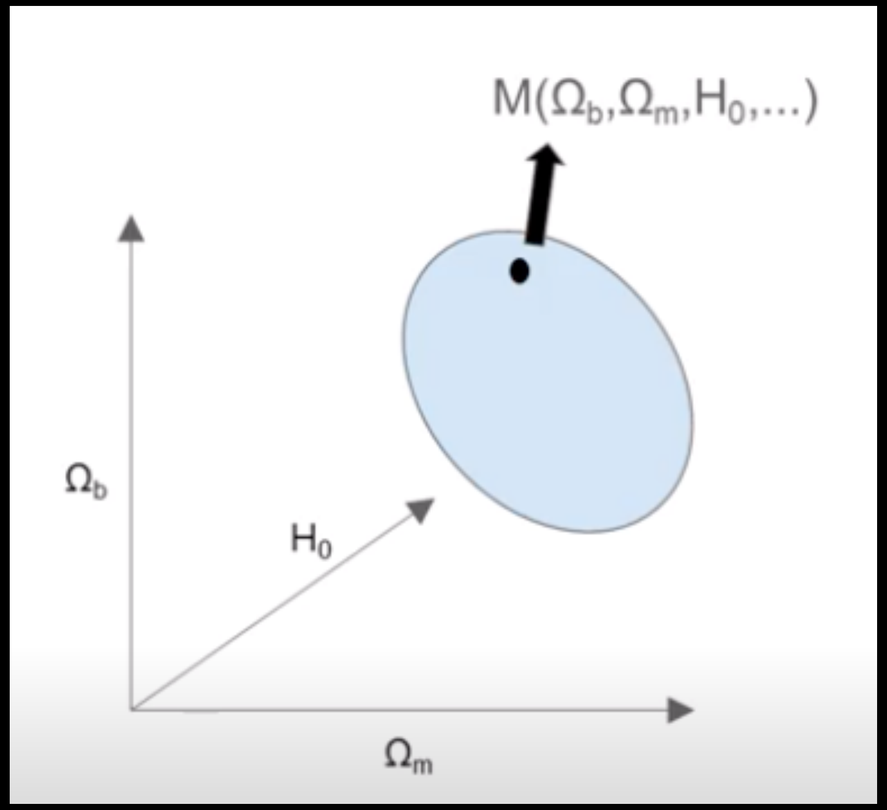

1. At given point in parameter space: generate a prediction based on your model in the parameter space.

How much that model prediction resembles the data?

2. Compute a probability function of the data given your prediction.

3. Use Bayes Theorem to get the posterior given some prior.

4. Given your sampler, move to the next point in the parameter space to evaluate a likelihood function.

Cosmology data sets

* Cepheid variables
* Type Ia SN
* Baryon Acoustic Oscillations
* Strong Lensing
* Light element abundances
* Globular cluster ages
* Cosmic Microwave Background
* Redshift Space Distortions
* Weak lensing
* Large scale structure
* Cluster counts
* 21cm line structure
* Ly-alpha forest in the quasar spectra

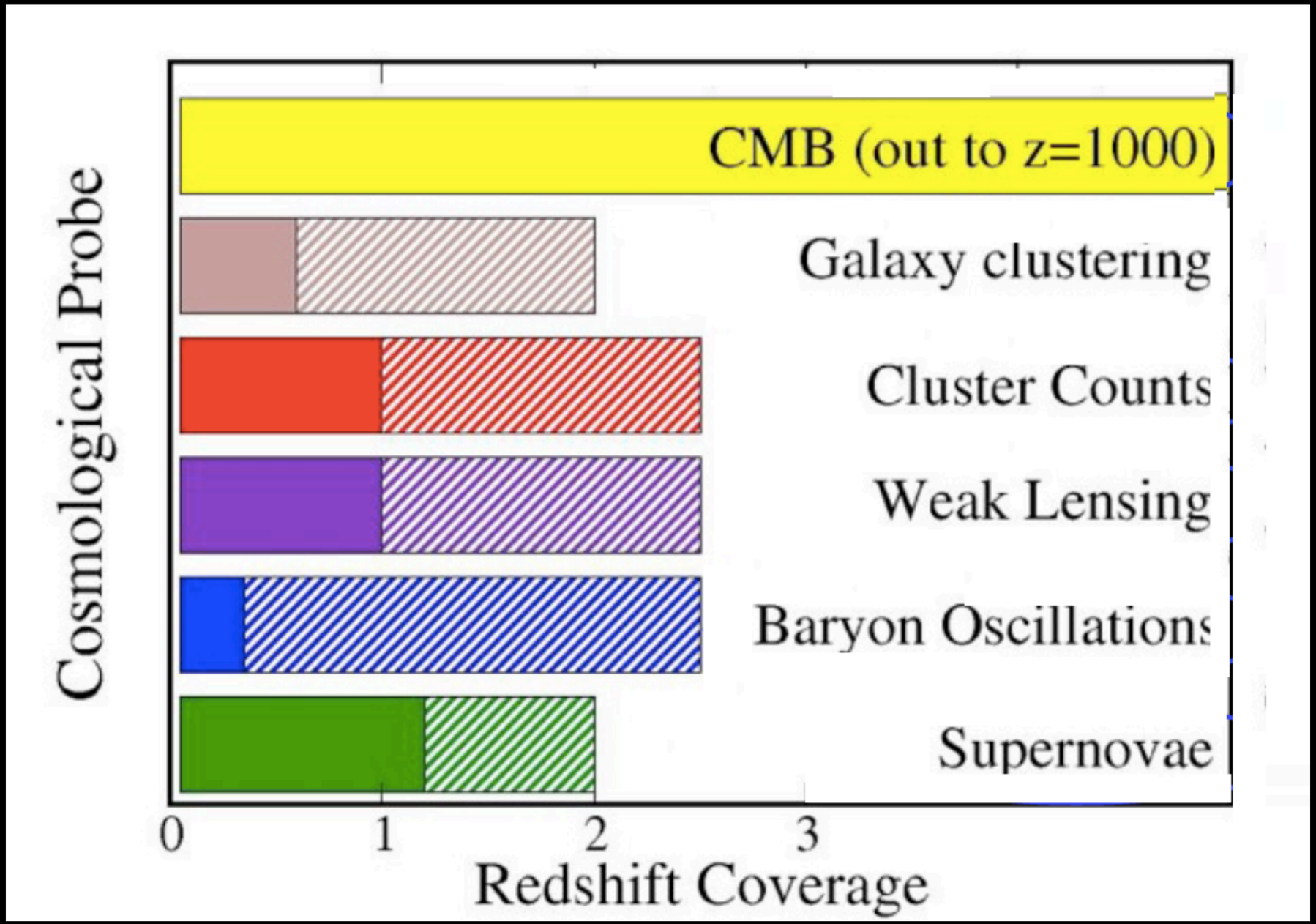
CMB (out to z=1000)
Galaxy clustering
Cluster Counts
Weak Lensing
Baryon Oscillations
Supernovae
Cosmological Probe
0
1
2
3
Redshift Coverage

Luminosity distances of the SNIa

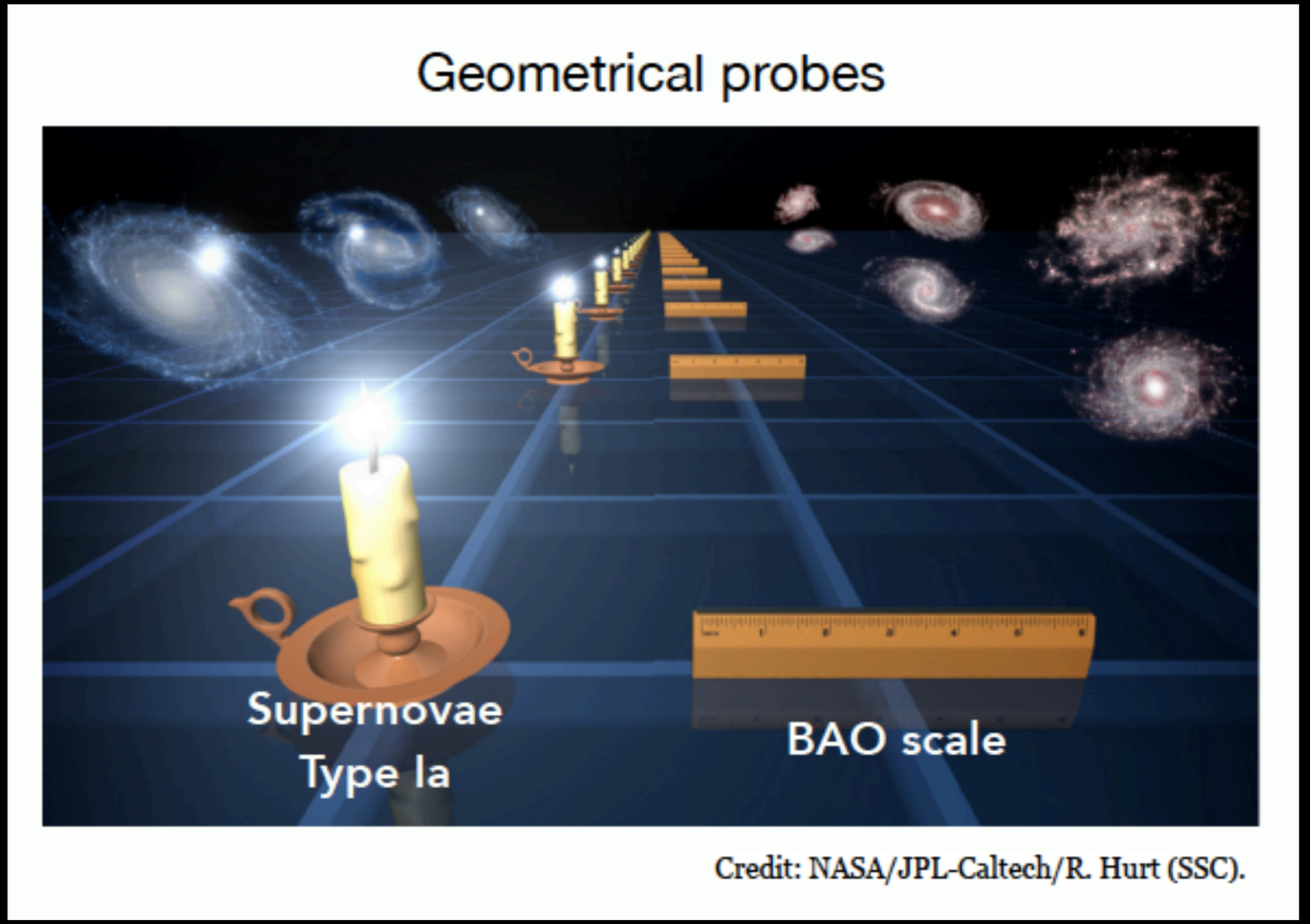

Luminosity distances of the SNIa ‘standard candles’

$$d_L(z) = \frac{c(1+z)}{H_0} \int_0^z \frac{dz'}{B(z')}$$

$$B(z') = (\Omega_{\phi_0} f(z'; m, z_*) + (1 - \Omega_{\phi_0})(1+z')^3)^{1/2}$$

$$\mu = m - M = 5(\log_{10} d_L(z) - 1)$$

Supernova Cosmology Project Union2.1 (Amanullah et al. 2010, Rubin et al. 2014)

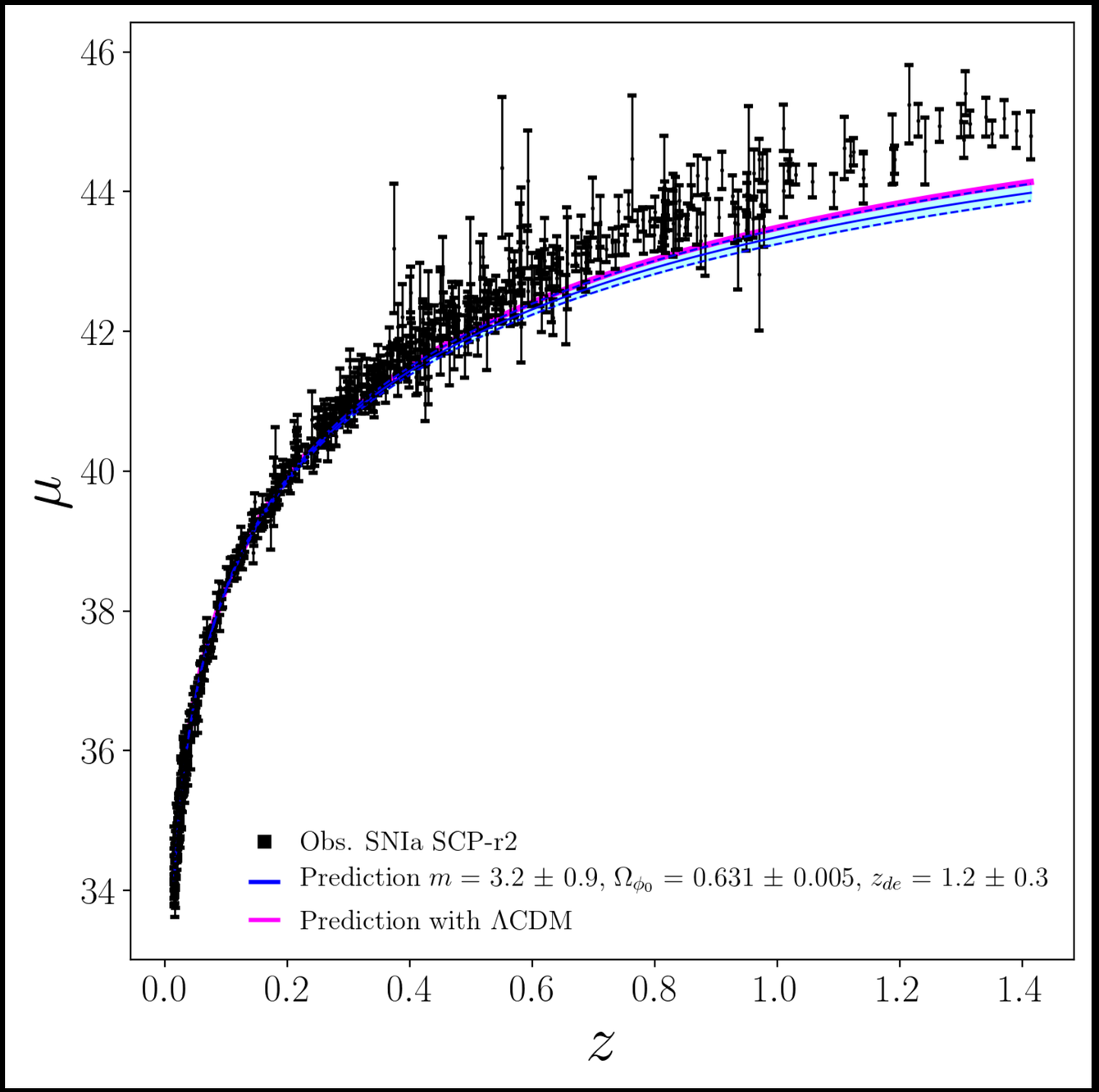

Constraining the model with observations

Distance modulus vs. redshift z computed with our model and Lambda CDM. We compare the theoretical predictions with observational data of SNIa from SCP2.1. We present our model, LambdaCDM and SNIa from SCP release in the blue line, magenta line and black points, respectively.

García +2020

BAO (baryon acoustic oscillations) ‘standard rulers’

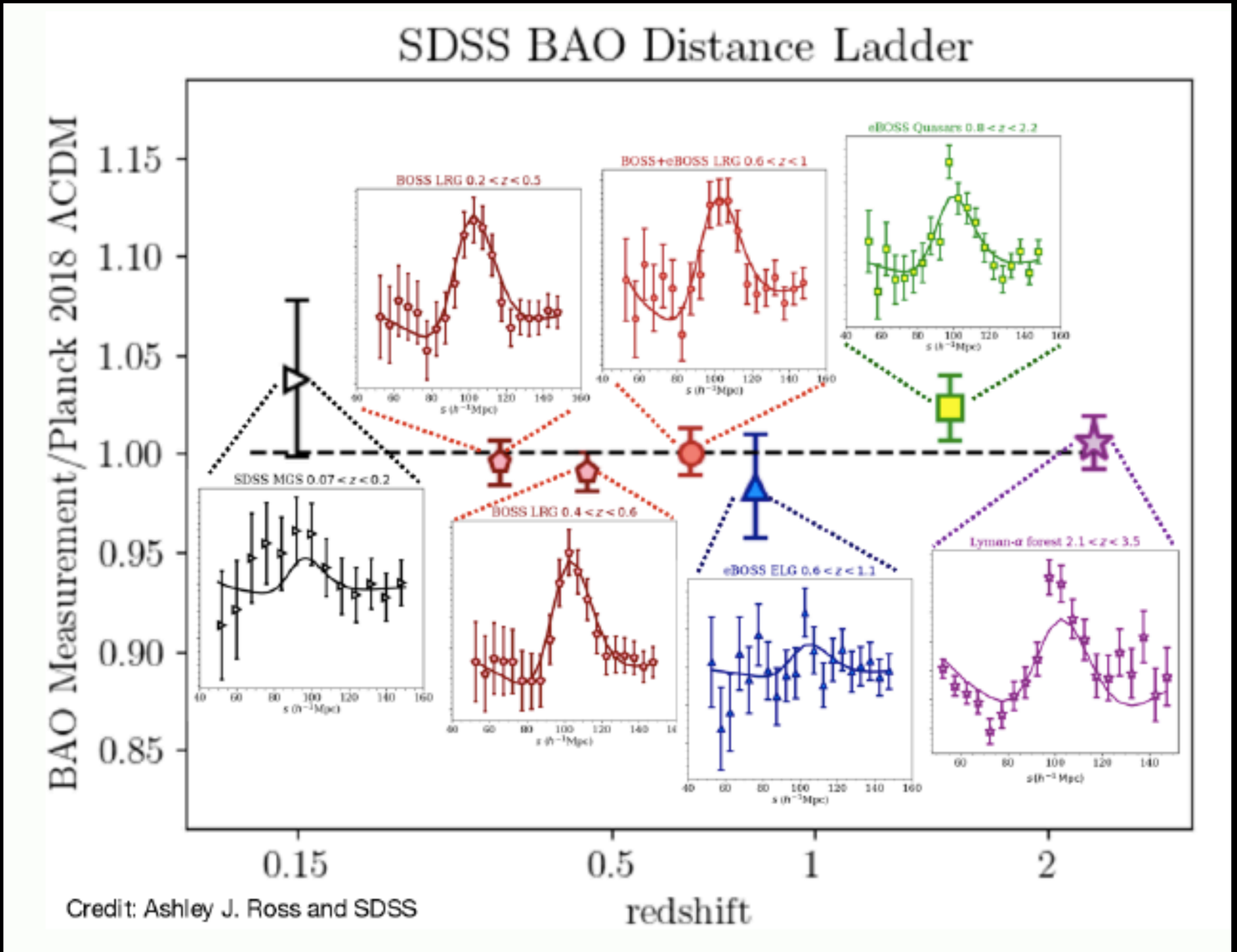

BAO (baryon acoustic oscillations)

$$r_s = \int_0^{t_*} \frac{c_s}{a(t)}\, dt = \frac{c}{\sqrt{3}} \int_0^{a_*} \frac{da}{a^2 H(a) \sqrt{1 + \frac{3\Omega_b}{4\Omega_\gamma}\, a}}$$

$$\Delta\theta_s = \frac{r_s}{d_A(z)} \quad \text{(transverse modes)}$$

$$D_V(z) \equiv \left[(1+z)^2 d_A(z) \frac{cz}{H(z)} \right]^{1/3}$$

BOSS -Baryon Oscillation Spectroscopic Survey- (Anderson et al. 2014)

6dF Galaxy Survey (Beutler et al. 2011)

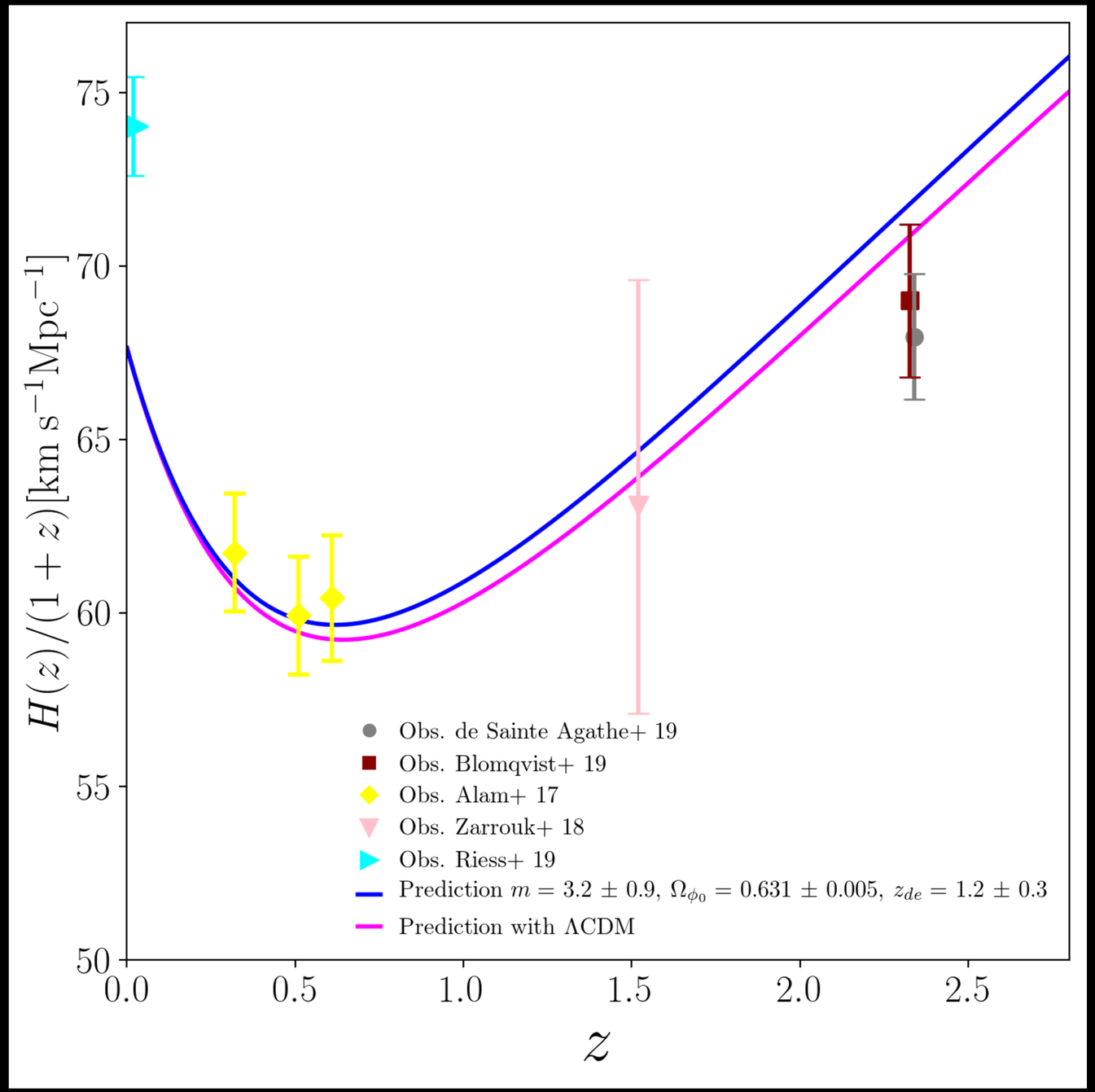

Constraining the model with observations

Prediction for H(z)/(1+z) as a function of redshift.BAO observations derived with BOSS DR12 from Alam2017 in yellow diamonds, from BOSS DR14 quasars by Zarrouk2018 in the pink inverted triangle, BOSS DR14 Lya autocorrelation at z = 2.34 with the grey circle, and BOSS DR14 joint constraint from the Lya auto-correlation and cross-correlation with quasars from Blomqvist 2019 in the dark red square. All the previous observations have computed with Planck 2018 cosmological parameters. The inferred Hubble measurement at z = 0 derived independently by Riess 2019 is shown with the cyan right tilted triangle.

García +2020

Cluster Count

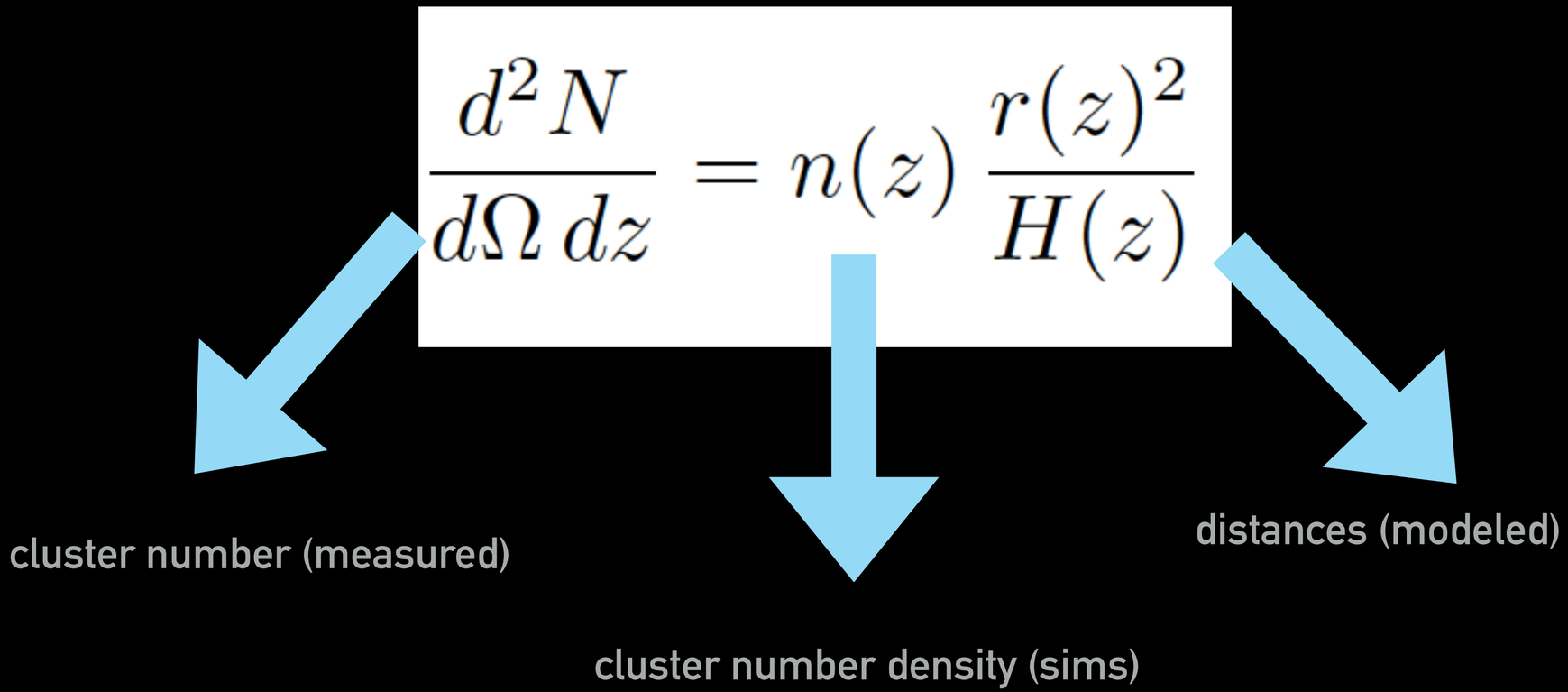

Planck Collaboration XXIV. Cosmology from Sunyaev-Zeldovich (Ade et al. 2018)

CMB (Cosmic Microwave Background)

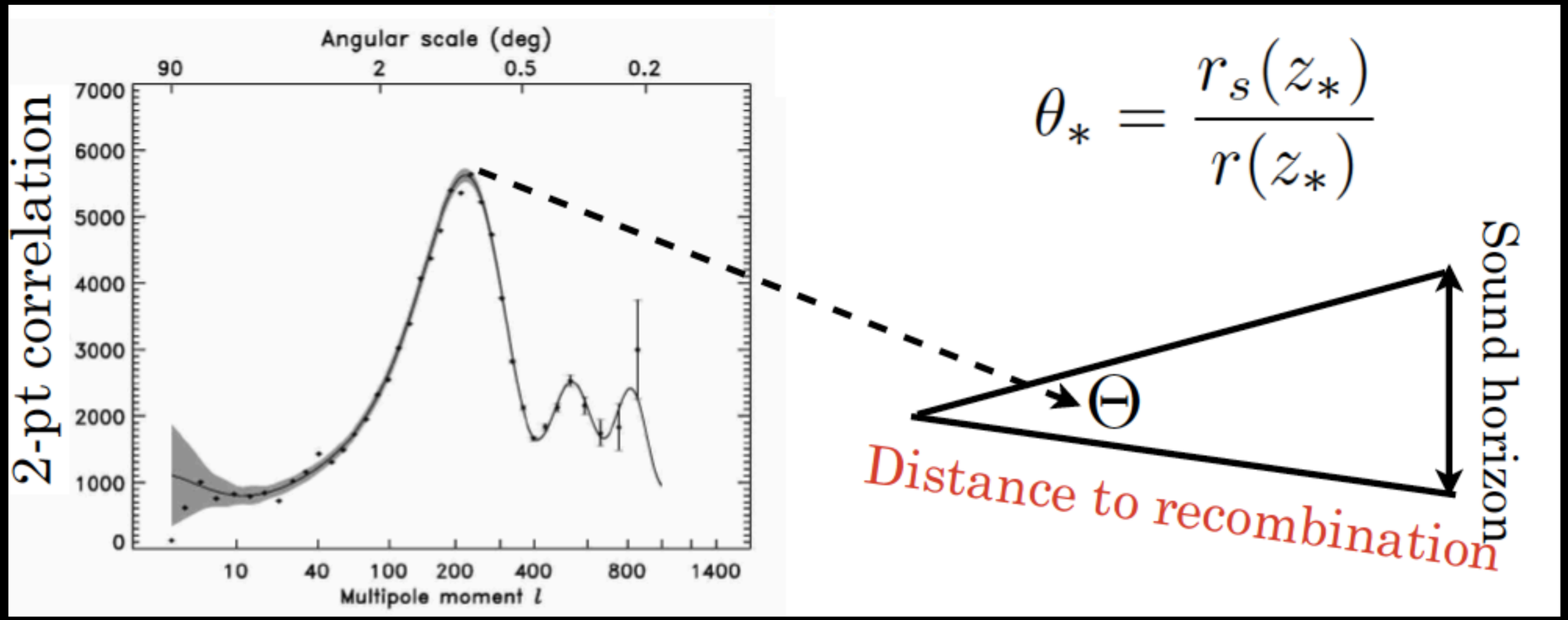

$$R \equiv \sqrt{\Omega_m H_0^2}\, r(z_*)$$

WMAP Collaboration (Komatsu et al. 2014), Planck Collaboration (Ade et al. 2015),

SPT (Schaffer et al. 2011)

Other cosmological probes

Weak gravitational lensing:

clustering (DM)

$$P_{\rm shear} \simeq \int_0^\infty W(r) P_{\rm matter}(r) dr$$

distances

H_0 prior

$$\rho_c = \frac{3H_0^2}{8\pi G}$$

$$\Omega \equiv \frac{\rho}{\rho_c} = \frac{8\pi G\rho}{3H_0^2}$$

but also,

- Gal-gal lensing
- Strong lensing
- RSD
- Peculiar velocities
- Hubble constant
- Cosmic voids
- Shear peaks
- Galaxy ages
- Redshift drift
- GRB & quasars

For instance, Riess et al. 2016

Hubble diagram with QSOs

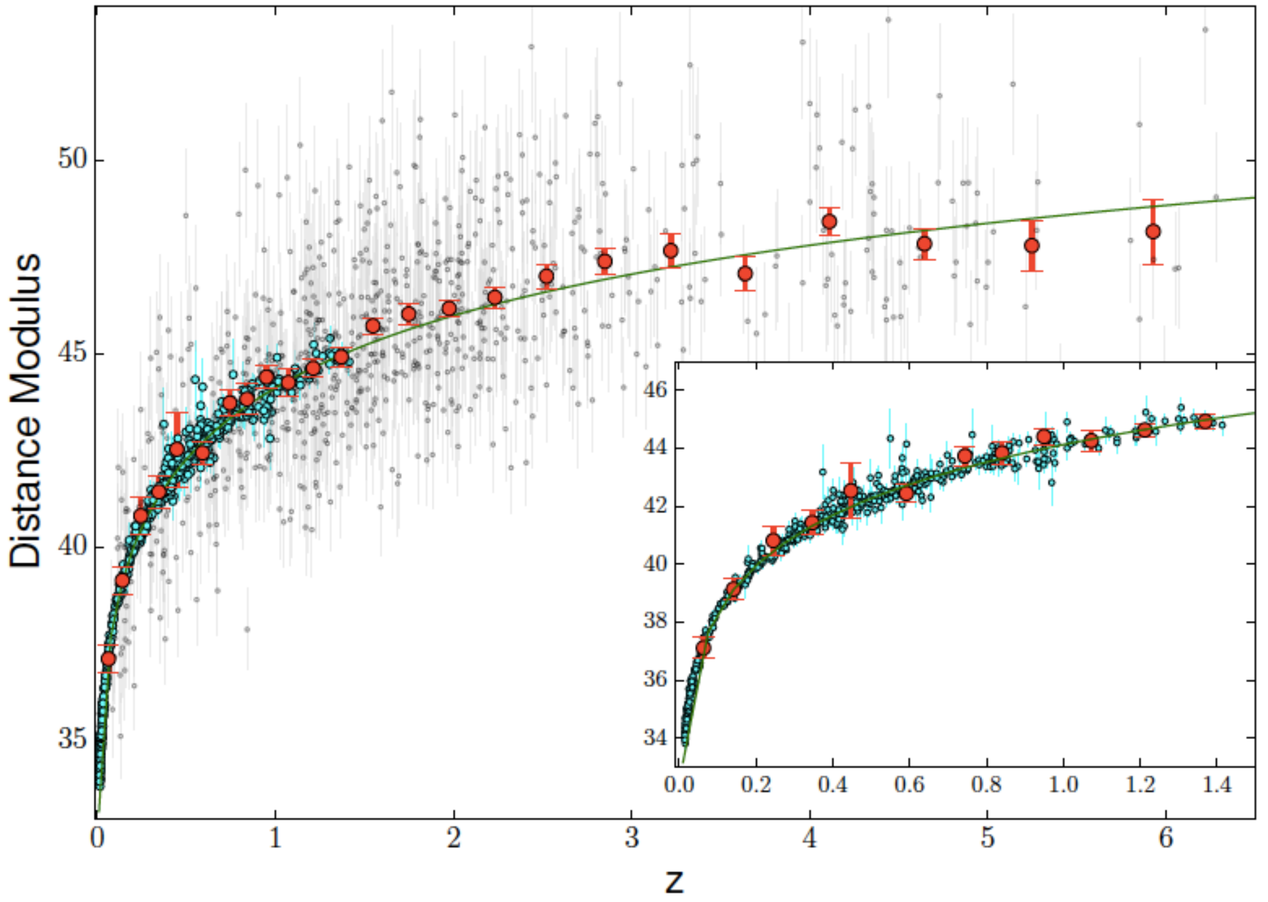

FIG. 5.— Hubble Diagram for the quasar sample (small gray points) and supernovae (cyan points) from the Union 2.1 sample (Suzuki et al. 2012). The large red points are quasar averages in small redshift bins. The inner box shows a zoom of the $z = 0 - 1.5$ range, in order to better visualize the match between the SNe and the quasar samples. The continuous line is obtained from a joint fit of the two samples assuming a standard ΛCDM cosmological model. The relative normalization between SNe and quasars is a free parameter of the fit, and it is estimated with an uncertainty lower than 1%.

Risaliti & Lusso 2015

Hubble diagram with QSOs

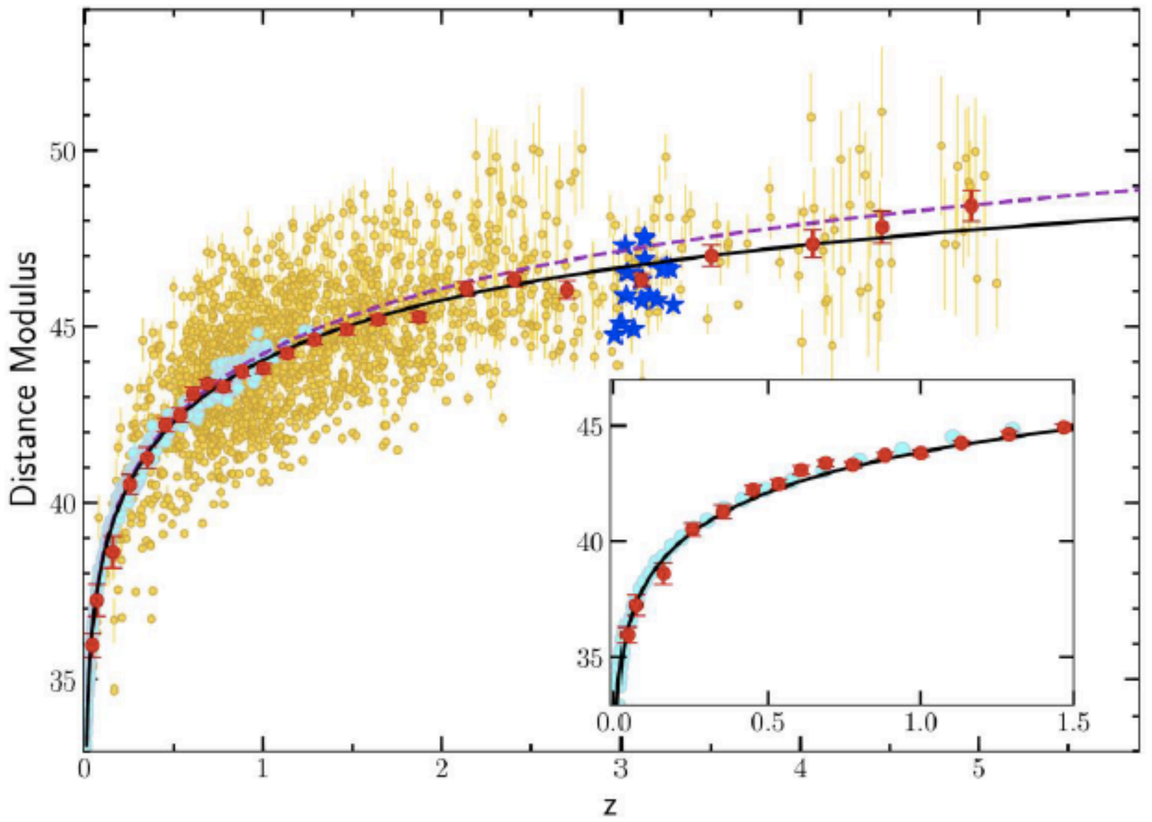

Figure 2: Hubble diagram of supernovae from the JLA survey[2] (cyan points) and quasars (yellow points). Red points represent the mean (and uncertainties on the mean) of the distance modulus in narrow redshift bins for quasars only. These averages are shown just for visualization and, as such, are not considered in the statistical analysis. The new sample of $z>3$ quasars with dedicated XMM-*Newton* observation is shown with blue stars. The inset is a zoom of quasar and supernovae averages in the common redshift range. The dashed magenta line shows a flat ΛCDM model with $\Omega_M=0.31\pm0.05$ fitting the $z<1.4$ data and extrapolated to higher redshifts. The black solid line is the best MCMC fit of the third order expansion of $\log(1+z)$.

Risaliti & Lusso 2018

Distance modulus SNIa vs. QSOs

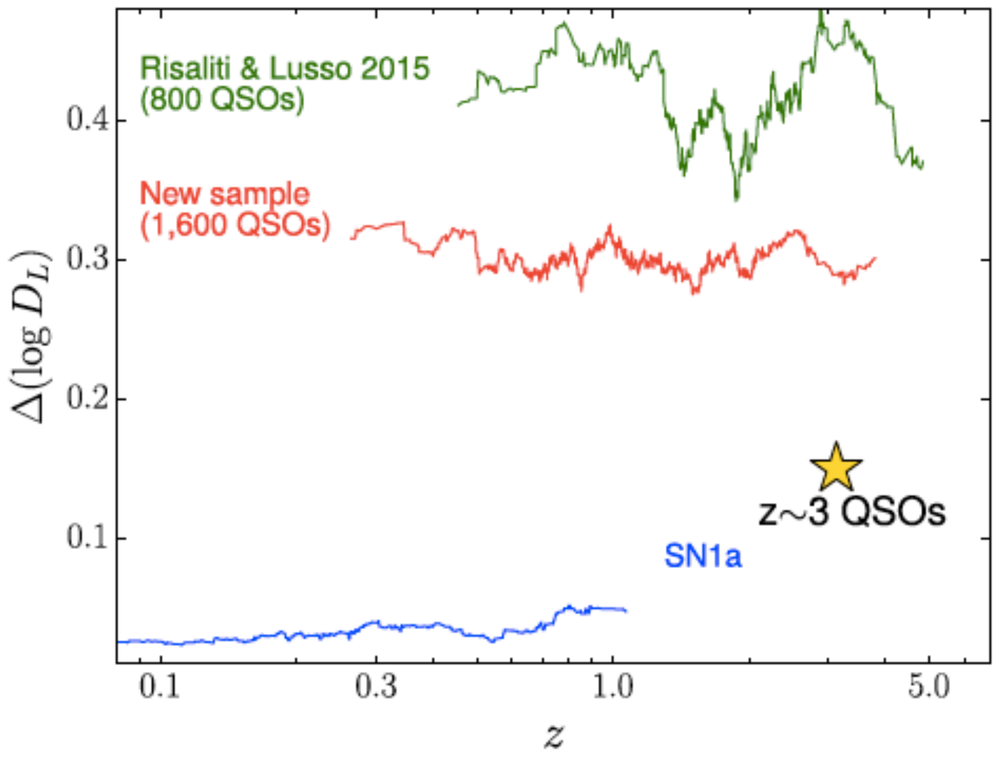

Supplementary Figure 6: Scatter on the Hubble Diagram as a function of redshift for the Type Ia supernovae from the JLA sample (blue line), the sample from our first work on the topic where we considered X-ray and UV flux measurements from the literature (green line), and the improved quasar sample presented in this manuscript (red line, Figs. 2 and 9). The star marks the value of the scatter on the Hubble Diagram obtained by considering the quasar sample at z=3.0-3.3 with dedicated XMM-*Newton* observations.

Risaliti & Lusso 2018

Hubble diagram with GRBs

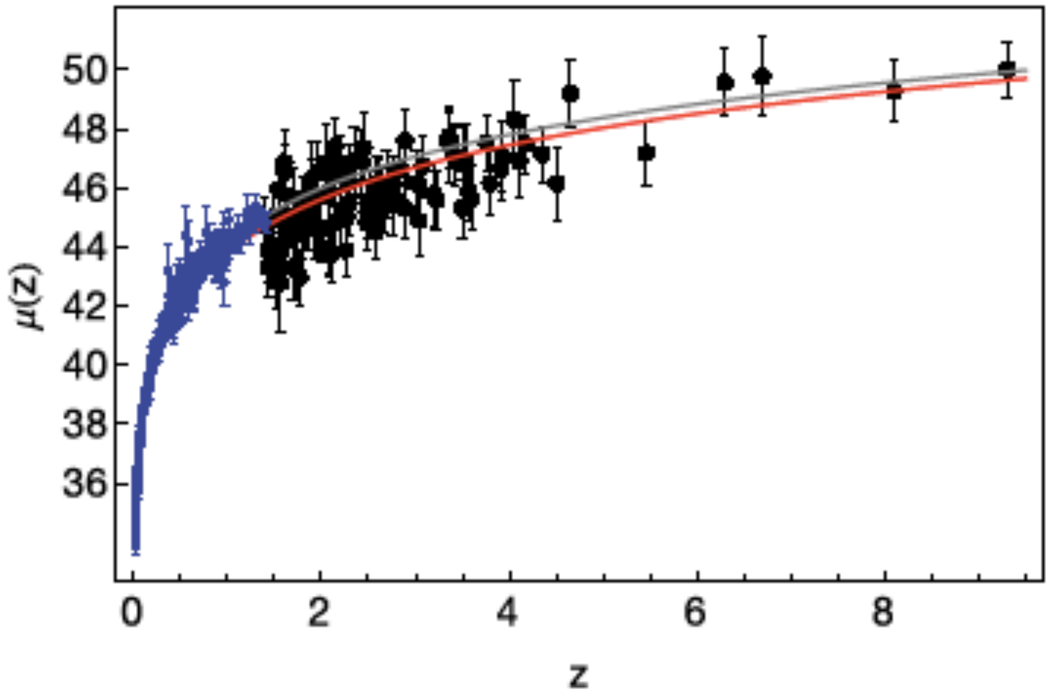

Fig. 6. Calibrated GRB Hubble diagram (black filled diamond) up to very high values of redshift, as constructed by applying the local regression technique with the Reichart likelihood: we show overplotted the behavior of the theoretical distance modulus $\mu(z) = 25 + 5 \log d_L(z)$ corresponding to the favored fitted CPL model (red line), with $w_0 = -0.29$, $w_1 = -0.12$, $h = 0.74$, $\Omega_m = 0.24$, and the standard ΛCDM model (gray line) with $\Omega_m = 0.33$, and $h = 0.74$. They are defined by Eqs. (12) and (21). The blue filled points at lower redshift are the SNIa data.

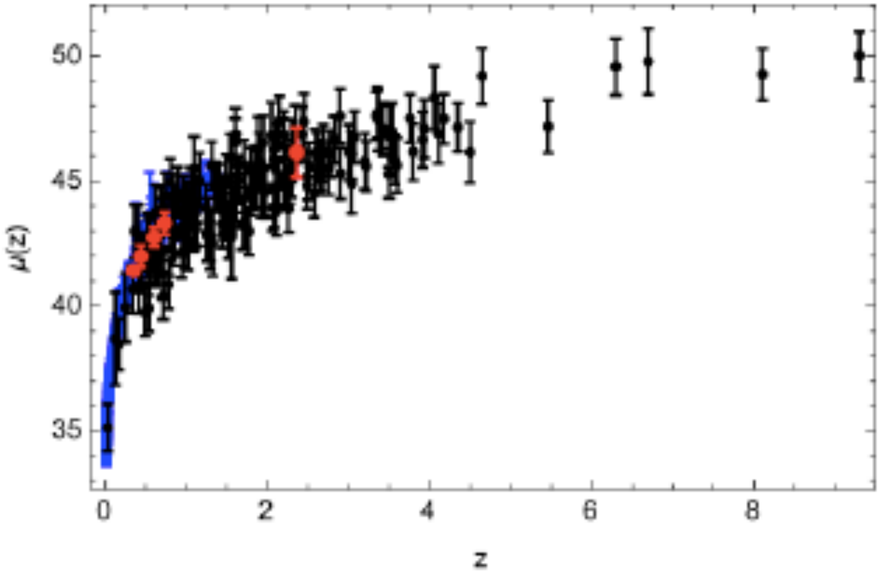

Fig. 7. GRB Hubble diagram (black points) is compared with the SNIa Hubble diagram (blue points) and with BAO data (red points).

Demianski +2017

Cosmology with FRBs

$$\mathrm{DM_{IGM}}(z) = \Omega_\mathrm{b} \frac{3H_0 c}{8\pi G m_\mathrm{p}} \times \int_0^z \frac{(1+z')\, f_\mathrm{IGM}(z') \left(Y_\mathrm{H} X_\mathrm{e,H}(z') + \frac{1}{2} Y_\mathrm{p} X_\mathrm{e,He}(z') \right)}{\left\{ \Omega_\mathrm{m} (1+z')^3 + \Omega_\Lambda (1+z')^{3[1+w(z')]} \right\}^{1/2}} dz',$$

$$\chi^2 = \sum_{i=1}^{n} \left[\frac{\mu_i^{obs}(z_i) - \mu_i^{th}(z_i)}{\sigma_{\mu_i^{obs}}} \right]^2$$

Hashimoto +2019

Table 2. Derived parameters of 27 robust FRBs with two cosmological assumptions.

(1)	(2)	(3)	(4)	(5)	(6)	(7)	(8)
		WMAP1			Planck15		
ID	$\mathrm{DM_{MW}}$ (pc $\mathrm{cm^{-3}}$)	Redshift	$\log L_\nu$ (erg $\mathrm{Hz^{-1}}$)	$\log w_\mathrm{int,rest}$ (ms)	Redshift	$\log L_\nu$ (erg $\mathrm{Hz^{-1}}$)	$\log w_\mathrm{int,rest}$ (ms)
010125	75.88	0.782±0.081	31.59±0.36	0.49±0.19	0.759±0.080	31.59±0.35	0.50±0.19
010312	54.88	1.231±0.098	32.37±0.08	0.98±0.04	1.203±0.096	32.37±0.08	0.99±0.04

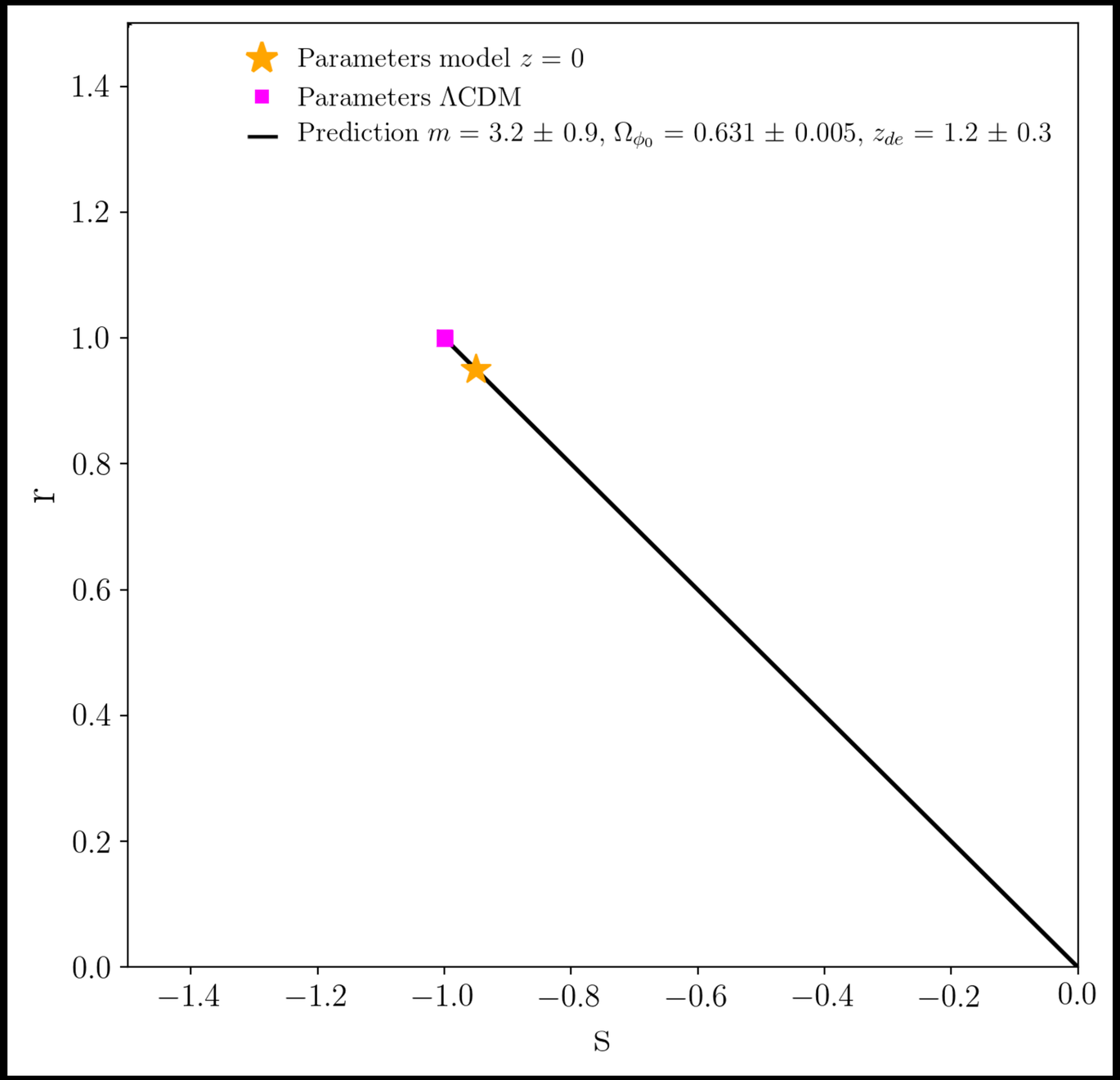

Statefinder parameters

Statefinder parameters space. The set of parameters today for Lambda CDM is presented with a purple square {r,s} = {1,-1}, while the values for our DE model are shown with the golden star. The black line exhibits the evolution with redshift of the Statefinder parameters given our model. The effective parametrization evolves from high redshift (early times) in the right lower side to the future in the left upper corner.

García +2020

Gravitational waves ‘standard sirens’

$$h''_{ij} + 2\mathcal{H}h'_{ij} + k^2 h_{ij} = 0\,,$$

$$d_L^{\rm gw} = \frac{(1+z)}{\sqrt{|\Omega_K|}}\,\mathrm{sinn}\left[c\int_0^z \frac{\sqrt{|\Omega_K|}}{H(z')}dz'\right],$$

$$\omega^2 = c_g^2 k^2 + m_g^2 + \sum_{n=3} \mathbb{A}_n k^n\,,$$

Amendola +2014a; Pettorino +2015; Raveri +2015

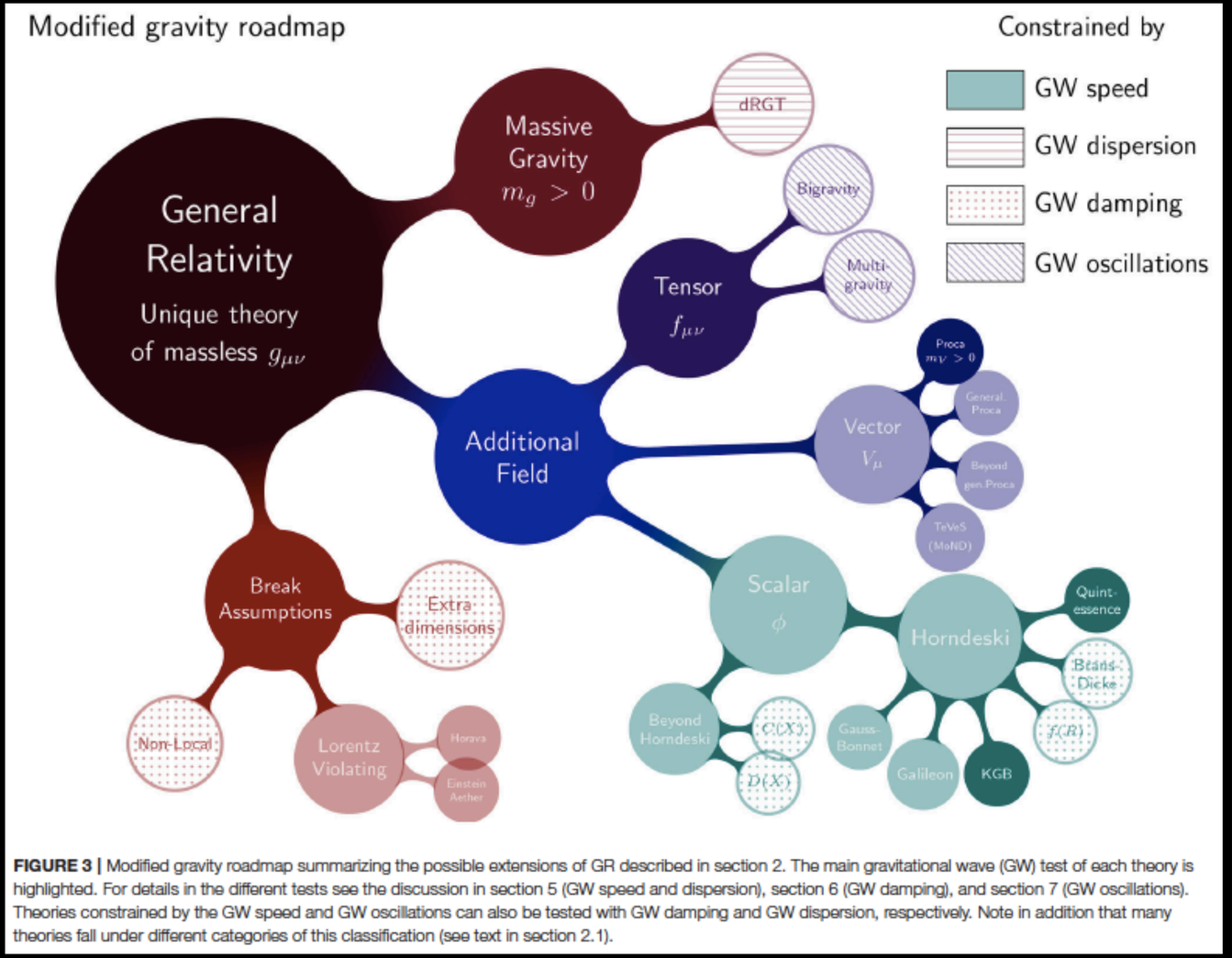

FIGURE 3 | Modified gravity roadmap summarizing the possible extensions of GR described in section 2. The main gravitational wave (GW) test of each theory is highlighted. For details in the different tests see the discussion in section 5 (GW speed and dispersion), section 6 (GW damping), and section 7 (GW oscillations). Theories constrained by the GW speed and GW oscillations can also be tested with GW damping and GW dispersion, respectively. Note in addition that many theories fall under different categories of this classification (see text in section 2.1).

Ezquiaga +2018

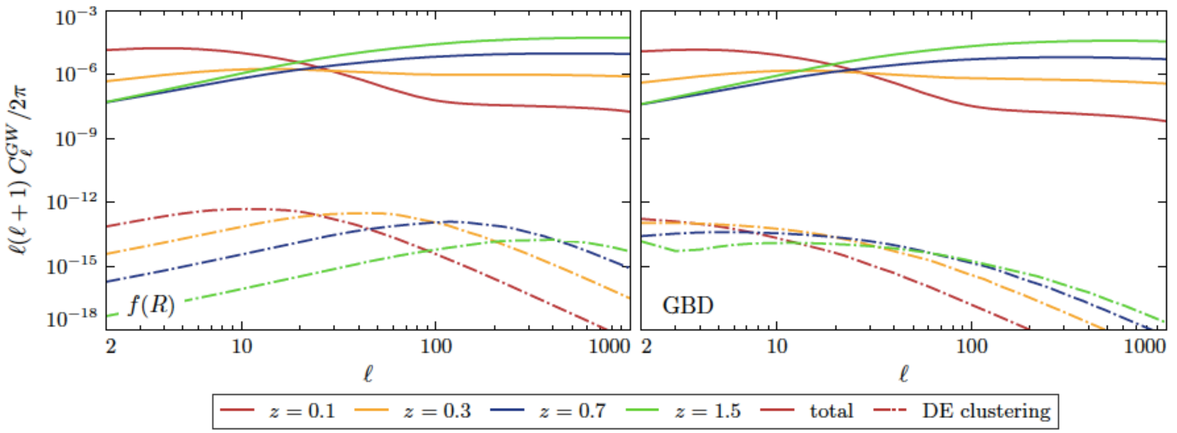

FIG. 1. The angular power-spectrum of gravitational-wave luminosity distance fluctuations in two representative MG models, $f(R)$ gravity and a Generalized Brans-Dicke (GBD) model. Different colors represent different redshifts, as shown in the legend. Solid line shows the total power-spectrum, dashed line the scalar field clustering component.

Garoffolo +2020

Constraints with ongoing surveys

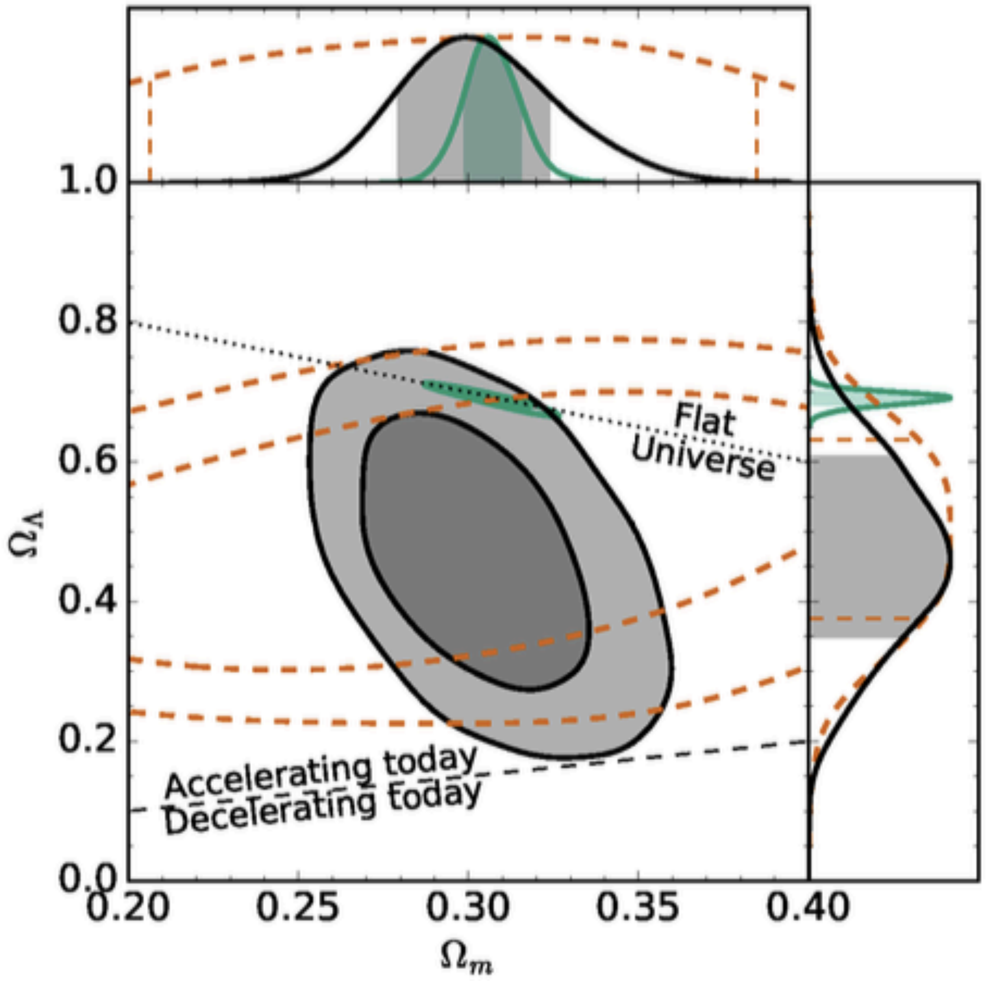

Figure 2: Constraints on dark energy density (Ω_Λ) and on matter density (Ω_m). Gray contours are constraints from DES data on weak gravitational lensing, large-scale structure, supernovae, and BAO. Green contours are the best available constraints, derived from CMB, supernovae, and BAO data. Contours represent 68% and 95% statistical confidence. (Y. Guo *et al.*, Phys. Rev. Lett. (2019))

DES

Padmanabhan 2019

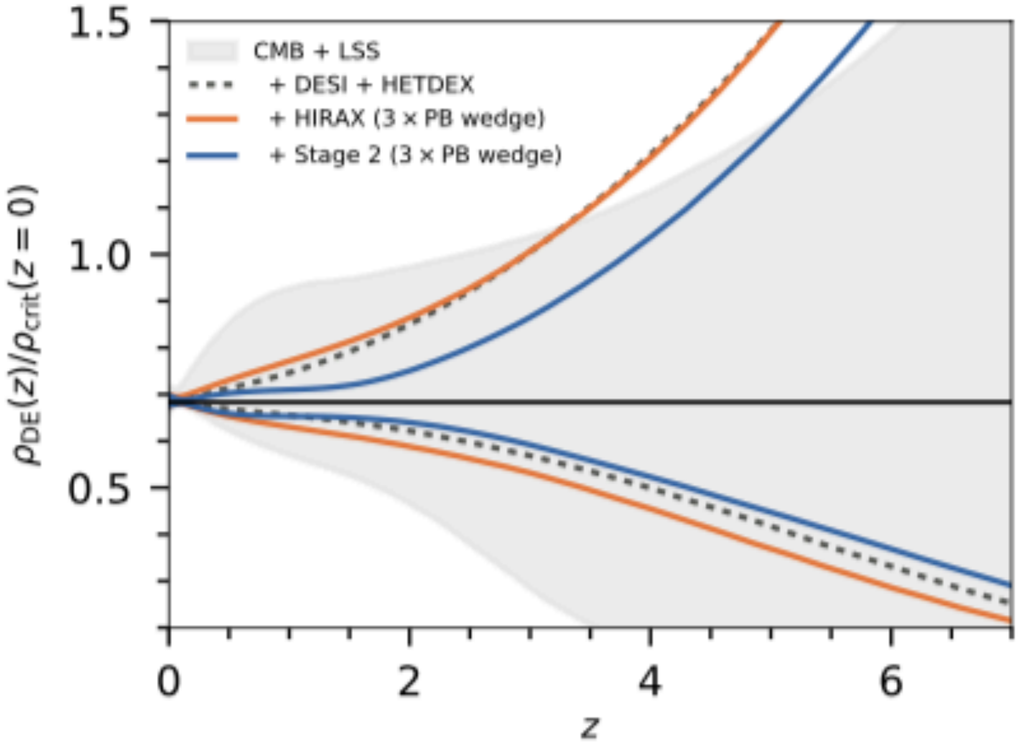

Figure 3. Forecast 95% CL constraints on $\rho_{DE}(z)$ in the Tracker model. The grey region shows the results for existing observations, a combination of CMB + large-scale structure constraints summarised in Table 1, while the solid/dashed lines show the combination of these existing data with forecasts for a selection of future experiments. The black horizontal line shows the fiducial ΛCDM model. Note that each line is for only CMB + LSS plus the experiment(s) listed in the legend, i.e. "+ HIRAX" should be read as "CMB + LSS + HIRAX", and does not include any other experiment.

Constraints with ongoing surveys

CMB + LSS

Planck CMB data

+

galaxy redshift survey & Lya forest (EBOSS).

Bull +2020

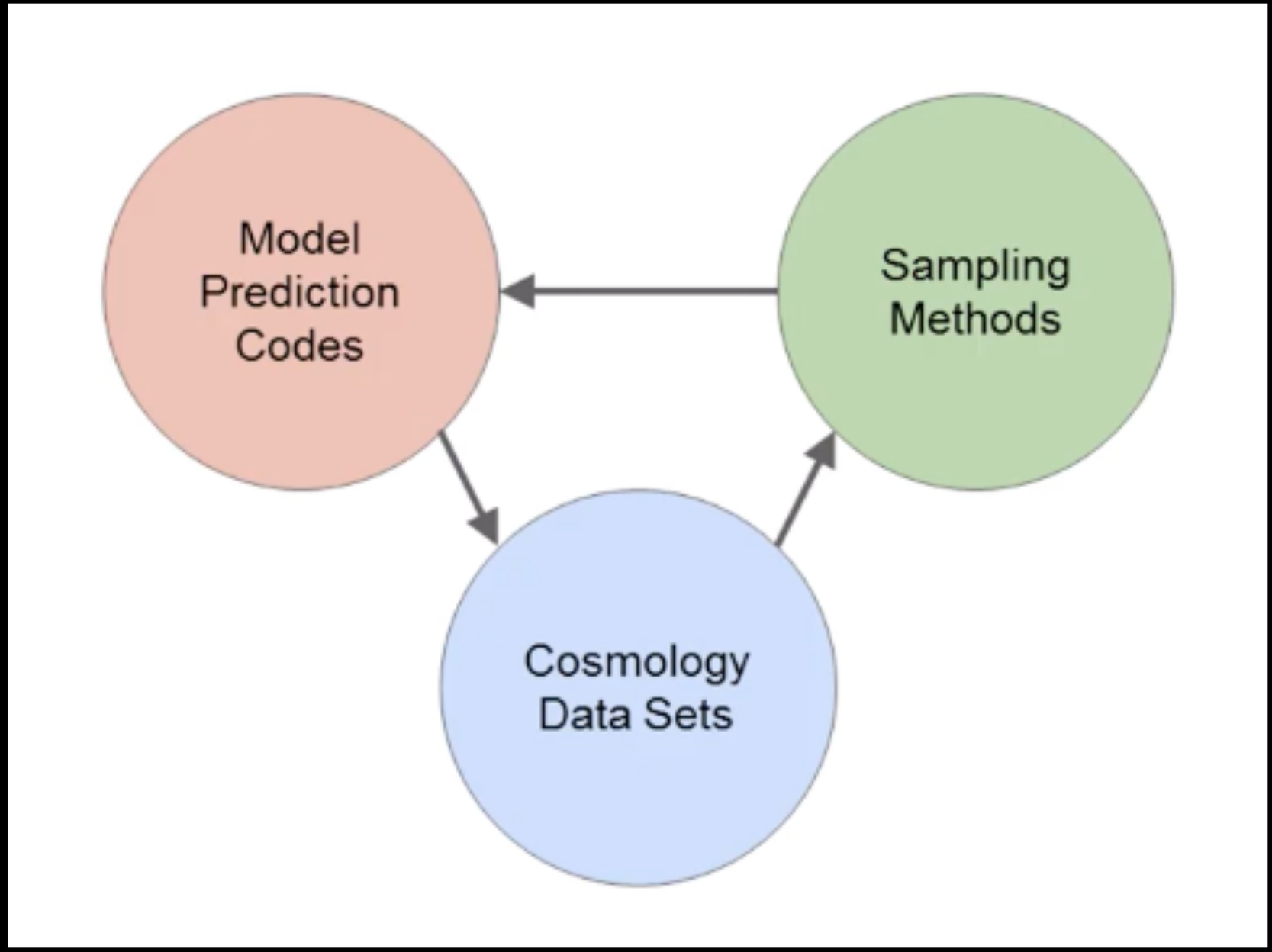
Model
Prediction
Codes
Sampling
Methods
Cosmology
Data Sets

Cosmology modelling: codes

* CAMB
* CLASS
* CosmoLike
* SNANA
* MGCCAMB
* MGCLASS
* IsItGR
* EFTCamb
* Colossus
* CosmoCalc
* AstroPy
* CosmoMC
* CosmoHammer
* CosmoSis
* Cosmolopy
* COBAYA

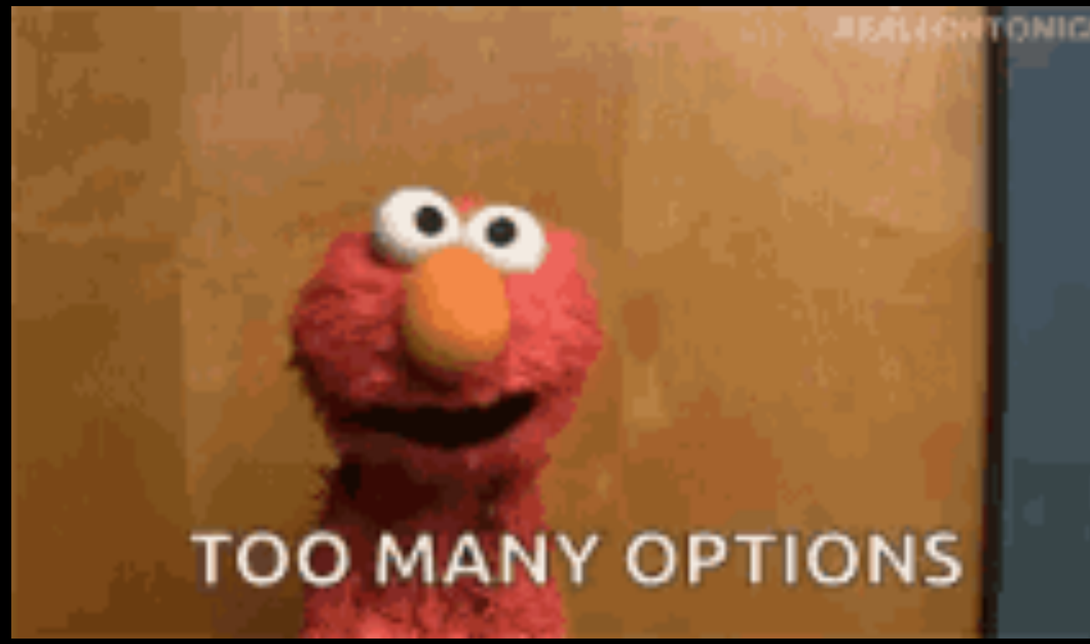

Thanks for your attention!

lgarciap@ecci.edu.co

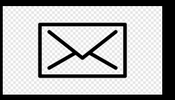

@PenLua

1.2 Dark energy projects

There are many observational projects to detect dark energy using the four dark energy probes: SN Ia, CMB, BAO and Weak Lensing (WL). Among them the Dark Energy Task Force (DETF) report [32] classifies the dark energy projects into four stages: Stage I–completed projects that already released data, Stage II–on-going projects, Stage III–intermediate-scale, near-future projects, and Stage IV–large-scale, longer-term future projects. Table 1 shows us the dark energy projects classified by probes and stages.

Probes	SN Ia	CMB	BAO	WL
Stage I	Higher-Z Team [10, 33], SNLS [34, 35, 36], ESSENCE [37, 38], NSF [39], CSP [40, 41], LOSS [42, 43, 44], SDSS [45, 46], SCP [21, 47, 48], CfA [49, 50], Palomar QUEST Survey [51]	COBE [52], TOCO [53], BOOMERang [54], Maxima [55], WMAP [14, 15, 16, 17]	2dFGRS [56], SDSS [57], 6dFGRS [58], WiggleZ [59]	CFHTLS [60, 61]
Stage II	Pan-STARRS1 [62], HST [63], KAIT [64]	Planck [65, 66, 67], SPT [68, 69], ACT [70]	SDSS II [71], SDSS III [72], BOSS [73, 74], LAMOST [75], WEAVE [76]	Pan-STARRS1, DLS [77, 78], KIDS [79]
Stage III	DES [80], Pan-STARRS4, ALPACA [81],ODI [82]	ALPACA, CCAT [83]	DES, HETDEX [84], BigBOSS [85], ALPACA, SuMIRe [86]	DES, Pan-STARRS4, ALPACA, ODI
Stage IV	LSST [87], WFIRST [88]	EPIC [89, 90], LiteBIRD [91, 92], B-Pol [93]	LSST, SKA [94], WFIRST, Euclid [95]	LSST, SKA, WFIRST, Euclid

Table 1: Dark energy projects. Classification is taken from ref. [32]. Note that the DETF report was published in 2006, and thus many Stage II projects are now shifted to Stage I.

Disclosure: this paper was published in 2012.

There are many new DE projects released or proposed.

Yoo +2012

Abstract

In this work, we explore upcoming cosmological proxies to constrain alternative cosmological models. We focus on a particular dark energy model with a non-negligible contribution during radiation domination epoch, and therefore, it could have introduced additional degrees of freedom on the Hubble parameter at that time. We consider probes that these candidates can be submitted in the future, and calculate the upper limits for the observables associated with dark energy models.